Paired box 5 increases the chemosensitivity of esophageal squamous cell cancer cells by promoting p53 signaling activity

Weiwei Zhang[1,2], Wenji Yan[3], Niansong Qian[4], Quanli Han[3], Weitao Zhang[5], Guanghai Dai[3]

[1]Chinese People's Liberation Army Medical School, Beijing 100853, China;
[2]Department of the Third Health Care, The Second Medical Center, Chinese People's Liberation Army General Hospital, Beijing 100853, China;
[3]Department of Oncology, The First Medical Center, Chinese People's Liberation Army General Hospital, Beijing 100853, China;
[4]Department of Oncology, The Hainan Medical Center, Chinese People's Liberation Army General Hospital, Sanya 572022, China;
[5]Cancer Center, Beijing Tongren Hospital Affiliated to Capital Medical University, Economic and Technological Development Zone, Beijing 100176, China.

Abstract

Background: Gene promoter methylation is a major epigenetic change in cancers, which plays critical roles in carcinogenesis. As a crucial regulator in the early stages of B-cell differentiation and embryonic neurodevelopment, the paired box 5 (*PAX5*) gene is downregulated by methylation in several kinds of tumors and the role of this downregulation in esophageal squamous cell carcinoma (ESCC) pathogenesis remains unclear.

Methods: To elucidate the role of *PAX5* in ESCC, eight ESCC cell lines, 51 primary ESCC tissue samples, and eight normal esophageal mucosa samples were studied and The Cancer Genome Atlas (TCGA) was queried. *PAX5* expression was examined by reverse transcription-polymerase chain reaction and western blotting. Cell apoptosis, proliferation, and chemosensitivity were detected by flow cytometry, colony formation assays, and 3-(4,5-dimethyl-2-thiazolyl)-2,5-diphenyl-2-H-tetrazolium bromide assays in ESCC cell lines with *PAX5* overexpression or silencing. Tumor xenograft models were established for *in vivo* verification.

Results: *PAX5* methylation was found in 37.3% (19/51) of primary ESCC samples, which was significantly associated with age ($P = 0.007$) and tumor-node-metastasis stage ($P = 0.014$). TCGA data analysis indicated that *PAX5* expression was inversely correlated with promoter region methylation ($r = -0.189$, $P = 0.011$ for cg00464519 and $r = -0.228$, $P = 0.002$ for cg02538199). Restoration of *PAX5* expression suppressed cell proliferation, promoted apoptosis, and inhibited tumor growth of ESCC cell lines, which was verified in xenografted mice. Ectopic *PAX5* expression significantly increased p53 reporter luciferase activity and increased p53 messenger RNA and protein levels. A direct interaction of *PAX5* with the p53 promoter region was confirmed by chromatin immunoprecipitation assays. Re-expression of *PAX5* sensitized ESCC cell lines KYSE150 and KYSE30 to fluorouracil and docetaxel. Silencing of *PAX5* induced resistance of KYSE450 cells to these drugs.

Conclusions: As a tumor suppressor gene regulated by promoter region methylation in human ESCC, *PAX5* inhibits proliferation, promotes apoptosis, and induces activation of p53 signaling. *PAX5* may serve as a chemosensitive marker of ESCC.

Keywords: PAX5; DNA methylation; Esophageal cancer; p53 signaling; Chemosensitivity

Introduction

Esophageal cancer (EC) is prevalent worldwide and is the sixth leading cause of cancer-related death.[1-3] Esophageal squamous cell carcinoma (ESCC) and esophageal adenocarcinoma are the main pathological subtypes of EC. In Asian countries, ESCC accounts for approximately 90% of all ECs.[4] Even with multimodal clinical treatments such as surgery, radiation treatment, and chemotherapy, the 5-year survival rate is low (20%).[5] ESCC also has poor sensitivity or is even resistant to many forms of chemotherapy.[6-8] There is considerable interest in finding new molecular targets for ESCC therapy as well as biomarkers that predict chemosensitivity and prognosis.

As a major epigenetic regulatory mechanism, promoter region hypermethylation contributes to inactivation of tumor suppressor genes, which plays a critical role in tumorigenesis.[9-12] For example, methylation of *TFPI-2*,[13] *RARB*, *P16INK4a*, *RASSF1*, *APC*, *RUNX3*, *p14ARF*,[14] and *PRSS8*[15] has been associated with the development of EC. Investigation of genes regulated by promoter region methylation in ESCC may facilitate identification of new biomarkers for diagnosis and therapy.[16-18]

The paired box 5 (*PAX5*) gene is located on chromosome 9p13, which encodes the Pax-5 protein. Pax-5 was originally documented as a B-cell-specific transcription

Access this article online

Quick Response Code:

Website: www.cmj.org

DOI: 10.1097/CM9.0000000000002018

Weiwei Zhang and Wenji Yan contributed equally to this work.

Correspondence to: Prof. Guanghai Dai, Department of Oncology, The First Medical Center, Chinese People's Liberation Army General Hospital, Beijing 100853, China
E-Mail: daigh60@sohu.com

Chinese Medical Journal 2022;135(5)
Received: 09-06-2021; **Online:** 21-02-2022 **Edited by:** Peifang Wei

factor with a crucial role in the early stages of B-cell differentiation and embryonic neurodevelopment.[19] *PAX5* mainly plays a tumor suppressor role and its inactivation favors cell transformation.[20-22] Promoter region hypermethylation of *PAX5* was reported in a set of cancer types that included head and neck squamous cell carcinoma,[23] gastric cancer,[21,22] hepatoma,[24] breast cancer,[25,26] and lung cancer.[27-30] Kurimoto *et al*[31] showed that methylation of the *PAX5* gene promoter region is correlated with poor survival outcomes and reduced cisplatin sensitivity in ESCC. Nevertheless, the exact role and involvement of *PAX5* in ESCC progression are poorly understood. Hence, this study further investigated the role of *PAX5* in ESCC.

Methods

Ethical approval

This study was approved by the Ethics Committee of the Chinese People's Liberation Army General Hospital (No. KY-2021-11-24-1). All patients signed a written informed consent form.

Primary human EC specimens and cell lines

A total of 51 cases of primary ESCC were surgically resected and eight cases of normal esophageal (NE) mucosa were collected from non-cancerous patients by biopsy under endoscopy. Additionally, eight ESCC cell lines (KYSE150, KYSE450, KYSE30, KYSE70, KYSE140, TE3, TE7, and TE10) were analyzed in this study. All EC cell lines were purchased from and identified by the Chinese Academy of Medical Sciences and Peking Union Medical College, and were established from primary EC and maintained in Roswell Park Memorial Institute 1640 medium (Invitrogen, Carlsbad, CA, USA) supplemented with 10% fetal bovine serum.

RNA isolation, semiquantitative reverse transcription-polymerase chain reaction (RT-PCR), and quantitative RT-PCR

Total RNA was extracted using Trizol reagent (Invitrogen). Complementary DNA (cDNA) was synthesized using the superscript III-reverse transcriptase kit (Invitrogen) in accordance with the manufacturer's instructions. Glyceraldehyde-3-phosphate dehydrogenase (GAPDH) was used as a control. Quantitative RT-PCR was performed on an ABI system (Foster City, CA, USA). Primer sequences of *PAX5* were: 5′-TGGCAGGTATTATGAGACAGG-3′ (forward) and 5′-CAGGCAAACATGGTGGGATT-3′ (reverse). GAPDH RT-PCR primer sequences were: 5′-GACCACAGTCCATGCCATCAC-3′ (forward) and 5′-GTCCACCACCCTGTTGCTGTA-3′ (reverse). Each experiment was repeated three times.

Bisulfite modification, methylation-specific PCR (MSP), and bisulfite sequencing (BSSQ)

Genomic DNA from ESCC cell lines and tissue samples was prepared using the proteinase K method. Normal lymphocyte (NL) DNA was prepared from blood lymphocytes of healthy donors by the proteinase K method. NL DNA was used as an unmethylated control and *in vitro*-methylated DNA (IVD) was used as a methylated control. IVD was prepared using SssI methylase (New England Biolabs, Ipswich, MA, USA) following the manufacturer's instructions. MSP and BSSQ primers were synthesized in accordance with a previous report.[24] MSP and BSSQ were performed as described previously.[32,33] To detect unmethylated (U) and methylated (M) alleles, MSP was performed using a 2720 Thermal Cycler (Life Technologies, Carlsbad, CA, USA). Cycle conditions were as follows: 95°C for 5 min; 35 cycles at 95°C for 30 s, 60°C for 30 s, and 72°C for 30 s; 72°C for 5 min. BSSQ products were amplified by primers that flanked targeted regions including MSP products. BSSQ was performed as described previously.[33] Cycle conditions were as follows: 95°C for 5 min; 35 cycles at 95°C for 30 s, 55°C for 30 s, and 72°C for 40 s; 72°C for 5 min. The primers for MSP flanked a 105 bp region located upstream of the *PAX5* transcription initiation site (−253 to −148 bp). These primers were as follows: PAX5-MF: 5′-AAATAAA-AATTCGGTTTGCGTTC-3′ (M-forward), PAX5-MR: 5′- AAACATACGCTTAAAAATCGCG-3′ (M-reverse); PAX5-UF: 5′- TAAAAATAAAAATTTGGTTTGTG-TTT-3′ (U-forward), PAX5-UR: 5′- TTAAAACATA-CACTTAAAAATCACA-3′ (U-reverse). BSSQ primers were as follows: 5′- TTTTTTTAAAAGTATTTG-TTTGGT-3′ (forward) and 5′- CACCTTCTATTAAAA-CATAC-3′ (reverse). Ten cytosine guanine dinucleotide (CpG) sites that spanned −297 and −136 bp regions were evaluated, which included the region analyzed by MSP.

5-Aza-2-deoxycytidine (DAC) treatment

Cells were treated with 2 μmol/L DAC (Sigma, St. Louis, MO, USA) in growth medium. The medium was changed every 24 h until 96 h, after which total RNA was extracted.

Plasmid construction and transfection

PAX5 expression vectors were subcloned into a pLenti6 lentiviral vector (Thermo Scientific, Wilmington, DE, USA). To establish cells with stable *PAX5* expression, we used ViraPower^{TM} Lentiviral Packaging Mix (Invitrogen) to package *PAX5* expression lentiviral vectors, which were used to infect KYSE150 and KYSE30 cells. Control cell lines were infected with empty lentiviral vectors. Successfully infected cells were selected using blasticidin (10 μg/mL; Invitrogen, 461120). The plasmids were transfected using Lipofectamine 3000 (Invitrogen, L3000015). pCMV6 and pcDNA3.1 plasmids (Era Biotech, Shanghai, China) were used for transient transfections. All constructs were verified by sequencing.

Knockdown of gene expression

To target all four transcripts of *PAX5*, we designed five short hairpin (sh) RNA molecules. We inserted these molecules into the plasmid genepharma U6 (pGPU6)/green fluorescent protein (GFP)/Neo vector (GenePharma, Shanghai, China) that was then used to transfect KYSE450 cells. The shRNA primer sequences were as follows: shRNA-1 (5′-GCCAGAGGATAGTGGAACTTG-3′),

shRNA-2 (5′-GGTAATTGGAGGATCCAAACC-3′), shRNA-3 (5′-GCCGACACCAACAAGCGCAAG-3′), shRNA-4 (5′-GGTGCTGGACCGCGTGTTTGA-3′), shRNA-5 (5′-GCAGACCACAGAGTATTCAGC-3′). Scramble shRNAs were sense: 5′-UUC UCC GAA GYC ACG UTT-3′; and antisense: 5′-ACG UGA CAC GUU CGG AGA ATT-3′). shRNA-3 was the most effective and used for subsequent experiments.

Colony formation assay

Cells were grown in six-well culture plates. Complete growth medium was changed every 48 h. After 2 weeks, the cells were fixed with 75% ethanol and stained with 0.2% crystal violet (Beyotime, Shanghai, China) to visualize and count.

Cell viability and proliferation assays

Cell lines were seeded in 96-well plates at 1.5×10^3 cells/well. A 3-(4,5-dimethyl-2-thiazolyl)-2,5-diphenyl-2-H-tetrazolium bromide (MTT) assay (KeyGEN Biotech, Nanjing, China) was used to measure cell viability. Quantification was performed using a spectrophotometer at a wavelength of 490 nm. Cell viability was measured on days 0, 1, 2, 3, and 4. p53 inhibitor Pifithrin-μ (20 μmol/L) (S2930, Selleckchem, Houston, TX, USA), which reduces affinity of p53 for B-cell lymphoma (Bcl) and Bcl-xL, and inhibits the binding of p53 to mitochondria,[34] was added at 12 h after seeding the cells. The MTT assay was then performed after 48 h. Half maximal inhibitory concentration (IC_{50}) was defined as the concentration of docetaxel or fluorouracil necessary to achieve 50% inhibition of cell growth. The IC_{50} value was calculated using SPSS 17.0 software (IBM, Armonk, NY, USA).

Bromodeoxyuridine (BrdU) proliferation assay and flow cytometry

BrdU proliferation assays of KYSE150, KYSE30, and KYSE450 cells were carried out using a fluorescein isothiocyanate (FITC) BrdU Flow Kit (BD Bioscience Pharmingen Inc., San Diego, CA, USA). Isolated cells were reseeded and incubated with BrdU; 1 mmol/L for 24 h. BrdU-incorporating cells (S phase) were analyzed at 72 h after seeding by following the manufacturer's instructions. Briefly, cells were fixed and permeabilized by BD Cytofix/Cytoperm Buffer (BD Bioscience Pharmingen Inc.). After 40 min of incubation with DNase at 37°C, cells were stained with a FITC-conjugated anti-BrdU monoclonal antibody (BD Bioscience Pharmingen Inc.). 7-Amino-actinomycin was added to each sample just prior to flow cytometric analysis using a FACSCalibur flow cytometer (BD Bioscience Pharmingen Inc.). The results are expressed as the percentage of cells in each phase of the cell cycle and were calculated as the mean ± standard deviation of three individual experiments.

Apoptosis assay

Cells were prepared using an Annexin V-FITC Apoptosis Detection Kit I (BD Bioscience Pharmingen Inc.). Then, the cells were analyzed by a FACSCalibur flow cytometer (BD Bioscience Pharmingen Inc.).

Western blot (WB) analysis

WB analysis was performed as described previously.[35] The antibodies used in the experiments were rabbit anti-PAX5 (#12709, 1:1000), mouse p53 (1C12) (#2524, 1:1000), rabbit poly adenosine disphosphate-ribose polymerase (PARP) (46D11) (#9532, 1:1000), rabbit anti-caspase-3 (#9661, 1:1000), rabbit anti-caspase-7 (#8438, 1:1000), rabbit anti-caspase-8 (#9496, 1:1000), rabbit anti-caspase-9 (#7237, 1:1000), PARP (#5625, 1:1000) (Cell Signaling Technology, Danvers, MA, USA); rabbit anti-p53 antibody (ab131442, 1:1000), rabbit anti-pro Caspase-3 antibody (ab32150, 1:1000), rabbit anti-pro Caspase-7 antibody (ab32067, 1:1000), rabbit anti-Pro Caspase-8 antibody (ab108333, 1:1000), rabbit anti-pro Caspase-9 (phospho T125) (ab138412, 1:500), and rabbit anti-PAX5 antibody (ab109443, 1:1000) (Abcam, Cambridge, UK). Rabbit anti-actin was used as a control (Cell Signaling Technology).

Dual luciferase reporter assay

Activity of the p53 signaling pathway was examined in ESCC cells using luciferase reporter p53-luc. KYSE150 and KYSE30 cells were transfected with pcDNA3.1-PAX5 or pcDNA3.1 (1×10^5 cells/well) in 24-well plates and cotransfected with the luciferase reporter plasmid (0.1 ng/well) and plasmid Renilla luciferase (pRL)-cytomegalovirus (CMV) (CMV promoter driving the renilla luciferase reporter) vector (2.5 ng/well) using Lipofectamine 3000. At 48 h post-transfection, the cells were harvested. The relative activity of luciferase was measured with the Dual-Luciferase Reporter Assay System (Promega, Madison, Wl, USA). For each experiment, the luciferase reporter assay was repeated three times.

Chromatin immunoprecipitation (ChIP) assay

ChIP assays were performed to examine the binding of Pax-5 protein to target DNA chromatin using a Red ChIP Kit (Diagenode, Seraing, Belgium). Chromatin DNA fragments were precipitated with 10 μg anti-PAX5 antibody (Abcam). The DNA was de-crosslinked and extracted from the DNA-protein complexes. ChIP-PCR was performed to confirm the presence of PAX5 bound on the p53 promoter, and immunoprecipitated DNA from the KYSE150-vector, KYSE150-PAX5, KYSE30-vector, and KYSE30-PAX5 cells were used as templates. The primer sequences were as follows: PAX5-F 5′-GTCCATTCCAT-CAAGTCCTG-3′ and PAX5-R 5′-TTGCTGACACAAC-CATGGCT-3′.

Xenografted mouse model

KYSE150 and KYSE30 cells stably infected with the pLenti6-PAX5 vector or empty pLenti6 vector (as control) were subcutaneously injected into the right dorsal flanks of 4-week-old male BALB/c nude mice (3×10^6 cells in 0.15 mL phosphate-buffered saline) ($n = 8$ per group). Tumor diameters were assessed at 10 days post-implantation and then every 2 days thereafter. Tumor volume, V (mm^3), was calculated using the formula: $V = L \times W^2/2$, where L represents the largest diameter (mm) and W represents the

smallest diameter (mm). The mice were euthanized on day 36 post-implantation and tumor weights were measured.

Immunostaining and in situ DNA nick end labeling

The xenograft tumor tissues were fixed in paraffin blocks and further detected by IHC staining. And IHC was performed on 4-μm thick serial sections derived from above formaldehyde-fixed paraffin blocks. Abcam anti-PAX5 antibody (Abcam) was diluted at 1:250 and Abcam anti-p53 antibody (Abcam) was diluted at 1:100. IHC was performed and evaluated as described previously.[35]

A terminal deoxynucleotidyl transferase-mediated deoxyuridinetriphate (dUTP)-digoxigenin nick end labeling (TUNEL) assay was performed using the Dead End Colorimetric TUNEL System (Promega). Clearly stained nuclei were considered TUNEL-positive apoptotic cells. After counting at least 1000 cells, the apoptotic index was calculated as the percentage of TUNEL-positive cells.

Statistical analysis

RNA sequencing (RNA-Seq) data of *PAX5* gene expression in ESCC and normal tissues were downloaded from the Genotype-Tissue Expression (GTEx) database (https://www.gtexportal.org/home/datasets) and The Cancer Genome Atlas (TCGA) (http://xena.ucsc.edu/, August 16, 2016), respectively. SPSS 22.0 (IBM) was used for all statistical analyses. Relationships between clinicopathological characteristics and methylation status were analyzed using the chi-squared test and Fisher's exact test. Continuous variables with normal distribution were assessed by the independent two-sample *t*-test. For xenografted tumors, the tumor volume growth curve was drawn using Graph Pad Prism 5.0 (GraphPad Software Inc., San Diego, CA, USA). Statistical significance was determined by two-sided tests and the null hypothesis was rejected at a $P < 0.05$ level.

Results

PAX5 is downregulated by promoter region hypermethylation in ESCC cell lines and primary tumors

The location of MSP and BSSQ primers around the transcription start site in the CpG island of the *PAX5* gene promoter region is shown in Figure 1A. The primer sequence was ever used in another study, and proved effective.[24] The MSP experiment showed no methylation of *PAX5* promoter region in KYSE450 cells, partial methylation in TE7, KYSE70, KYSE140, and TE10 cells, and complete methylation in KYSE30, KYSE150, and TE3 cells [Figure 1B]. The BSSQ experiment confirmed the above results. Figure 1C shows that *PAX5* promoter region was entirely unmethylated in KYSE450 cells, partially methylated in TE10 cells, and completely methylated in KYSE150 cells. Semiquantitative RT-PCR was used to measure the expression level of *PAX5* in the eight ESCC cell lines. High expression of *PAX5* was found in KYSE450 cells with *PAX5* promoter region unmethylated, while the expression of *PAX5* was found silenced or reduced in all another seven cell lines. Reduced expression of *PAX5* was found in TE7, KYSE70, KYSE140, and TE10 cells with *PAX5* promoter region methylated partially, whereas loss of *PAX5* expression was found in KYSE150, KYSE30, and TE3 cells with *PAX5* promoter region methylated completely [Figure 1D]. Thus, the expression of *PAX5* in ESCC cell lines was inversely correlated with promoter region methylation. Furthermore, we treated ESCC cells with demethylation agent DAC. In KYSE150 and KYSE30 cells with *PAX5* promoter region methylated completely, the addition of DAC led to restoration of *PAX5* expression [Figure 1E]. Conversely, expression of *PAX5* was equally high in *PAX5* promoter region-unmethylated KYSE450 cells with or without DAC treatment. The above results revealed that expression of *PAX5* was regulated by promoter region methylation.

We further detected the methylation status of *PAX5* in ESCC cancer tissues. *PAX5* promoter region methylation was observed in 37.3% (19/51) of cancer specimens, whereas no methylation of *PAX5* promoter region was found in all eight NE mucosa samples [Figure 2A]. Hypermethylation of *PAX5* promoter region was significantly associated with a young age ($P = 0.007$) and advanced tumor-node-metastasis (TNM) stage ($P = 0.014$) [Table 1]. No significant association was found between *PAX5* promoter methylation and sex, or tumor location (all $P > 0.05$).

To further investigate the correlation of promoter region methylation and expression of *PAX5*, we explored GTEx and TCGA (http://xena.ucsc.edu/) databases. We analyzed RNA-Seq data of 179 ESCC tissue samples and eight adjacent tissue samples. Perhaps due to the sample size limitation of adjacent tissue samples, no statistical significance was found between the 179 ESCC cancer tissue samples and the eight adjacent tissue samples ($P = 0.756$; independent two-sample *t*-test) or between the eight cancer tissue samples and paired adjacent tissue samples from the same patients ($P = 0.195$; paired two-sample *t*-test) in *PAX5* messenger RNA (mRNA) levels [Figure 2B]. Nevertheless, *PAX5* expression was negatively correlated with promoter hypermethylation ($r = -0.189$, $P = 0.011$ for CpG site cg00464519; and $r = -0.228$, $P = 0.002$ for CpG site cg02538199) (cg00464519 and cg02538199 are two CpG sites in *PAX5* promoter region) [Figure 2C]. Among these patients, 16 patients had Infinium Human Methylation 450 (HM450) detection data both in cancer and matched adjacent ESCC samples, the methylation levels were significantly higher in cancer tissues than in adjacent tissues ($P = 0.003$ for cg00464519, $P = 0.011$ for cg02538199) [Figure 2D]. However, perhaps because of the cutoff value, which was automatically generated by the system, no association was found between *PAX5* mRNA expression and 5-year overall survival (OS) ($n = 175$, $P = 0.951$) [Figure 2E]. No associations were found between CpG island methylation of *PAX5* promoter region and OS ($n = 181$, $P = 0.423$ for cg00464519, $P = 0.536$ for cg02538199) [Figure 2F] in this cohort.

Restoration of PAX5 expression suppresses ESCC cell growth

To investigate whether *PAX5* has a tumor-suppressive effect, colony formation assays were performed to evaluate

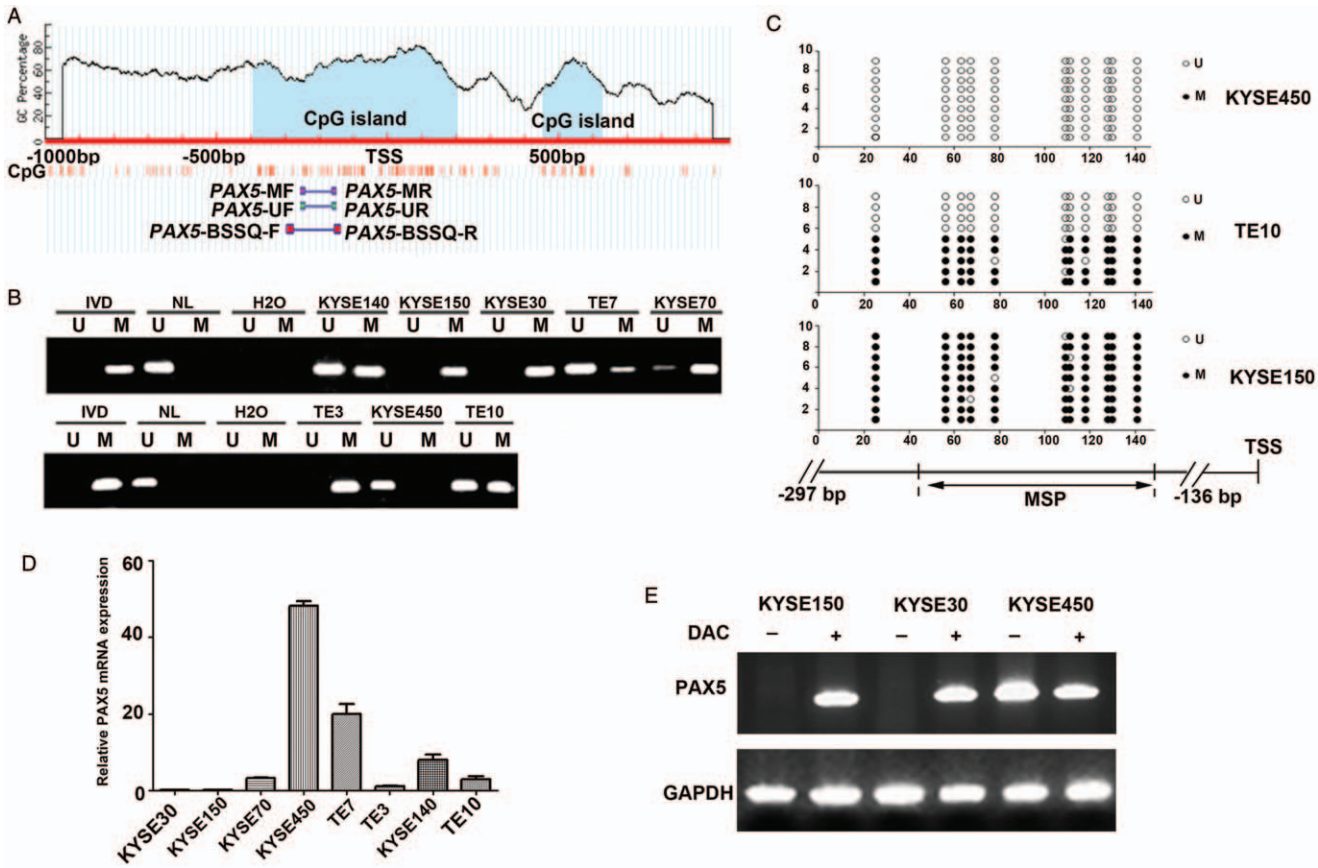

Figure 1: *PAX5* expression is inversely correlated with DNA methylation in ESCC cell lines. (A) Diagram of CpG islands in the *PAX5* promoter region generated using the MethPrimer tool (http://www.urogene.org/cgi-bin/methprimer/methprimer.cgi). (B) Methylation status of *PAX5* promoter region was detected by MSP in EC cell lines. Primer efficiency was confirmed using IVD as a positive control and NL DNA as a negative control. (C) BSSQ analysis of *PAX5* promoter region was performed in KYSE450, TE10, and KYSE150 cell lines. Double-headed arrow indicates the region (105 bp) of CpG islands examined by MSP. Filled circles denote methylated CpG sites in *PAX5* promoter region CpG islands. Open circles represent unmethylated CpG sites. BSSQ focused on the 161-bp (−297 to −136 bp) CpG islands upstream of the *PAX5* transcription start site. (D) mRNA expression of *PAX5* was analyzed by quantitative RT-PCR in eight ESCC cell lines (KYSE30, KYSE150, KYSE70, KYSE450, TE7, TE3, KYSE140, and TE10). (E) mRNA expression levels of *PAX5* were analyzed by semiquantitative RT-PCR in KYSE150, KYSE30, and KYSE450 cell lines following exposure (+) to DAC for 96 h or the negative control (−). BSSQ: Bisulfite sequencing; BSSQ-F: Bisulfite sequencing forward primer; BSSQ-R: Bisulfite sequencing reverse primer; CpG: Cytosine guanine dinucleotide; DAC: 5-Aza-2-deoxycytidine; EC: Esophageal cancer; ESCC: Esophageal squamous cell cancer; GAPDH: Glyceraldehyde-3-phosphate dehydrogenase; IVD: *In vitro*-methylated DNA; M: Methylated alleles; MF: MSP forward primer; MR: MSP reverse primer; mRNA: Messenger RNA; MSP: Methylation-specific polymerase chain reaction; NL: Normal lymphocyte; *PAX5*: Paired box 5; U: Unmethylated alleles; UF: Unmethylated forward primer; UR: Unmethylated reverse primer; RT-PCR: Reverse transcription-polymerase chain reaction; TSS: Transcriptional start site.

the effect of *PAX5* on clonogenicity. Restoration of *PAX5* expression in KYSE150 and KYSE30 cell lines was confirmed by WB [Figure 3A]. Colony numbers of KYSE150 and KYSE30 cells transfected with the PAX5 expression vector were decreased significantly compared with those in the control group (125.18 ± 25.39 *vs.* 317.72 ± 39.07 for KYSE150, $t = -7.16$, $P = 0.002$; 152.97 ± 20.06 *vs.* 380.54 ± 83.98 for KYSE30, $t = -4.58$, $P = 0.010$). Knockdown of *PAX5* in KYSE450 cells resulted in a significant increase in colony numbers (303.18 ± 37.28 *vs.* 189.45 ± 24.23, $t = 4.43$, $P = 0.011$) [Figure 3B], which confirmed the inhibitory effect of *PAX5* on clonogenicity. Furthermore, we performed MTT cell viability assays. The OD values were 1.31 ± 0.01 *vs.* 2.36 ± 0.01 for KYSE150 cells ($P < 0.001$) and 1.68 ± 0.03 *vs.* 2.44 ± 0.06 for KYSE30 cells ($P < 0.001$) with or without re-expression of *PAX5*. The OD values were 2.72 ± 0.06 *vs.* 2.27 ± 0.06 ($P = 0.001$) with or without knockdown of *PAX5* in KYSE450 cells. Cell viability decreased upon restoration of *PAX5* expression in KYSE150 and KYSE30 cells and increased after knockdown of *PAX5* in KYSE450 cells (Figure 3C; $n = 3$ experiments performed as triplicates). Additionally, we assessed the effect of DAC treatment on KYSE150, KYSE30, and KYSE450 cell proliferation by a BrdU proliferation assay that provides an accurate determination of cells in S-phase of the cell cycle through flow cytometry. Upregulation of *PAX5* in KYSE150 and KYSE30 cells after DAC treatment was confirmed by WB, whereas no change was found in KYSE450 cells before or after DAC treatment [Figure 3D]. Cells in S-phase of the cell cycle were lower among DAC-treated KYSE150 and KYSE30 cells compared with control groups ($[25.19 \pm 1.73]\%$ *vs.* $[36.36 \pm 1.80]\%$ for KYSE150, $P = 0.011$; $[27.23 \pm 1.33]\%$ *vs.* $[35.53 \pm 1.86]\%$ for KYSE30, $P = 0.022$), whereas there was no significant difference in KYSE450 cells with or without DAC treatment ($[36.25 \pm 2.13]\%$ *vs.* $[35.59 \pm 1.37]\%$, $P = 0.808$) [Figure 3E]. These results suggested that restored expression of *PAX5* inhibited ESCC cell proliferation.

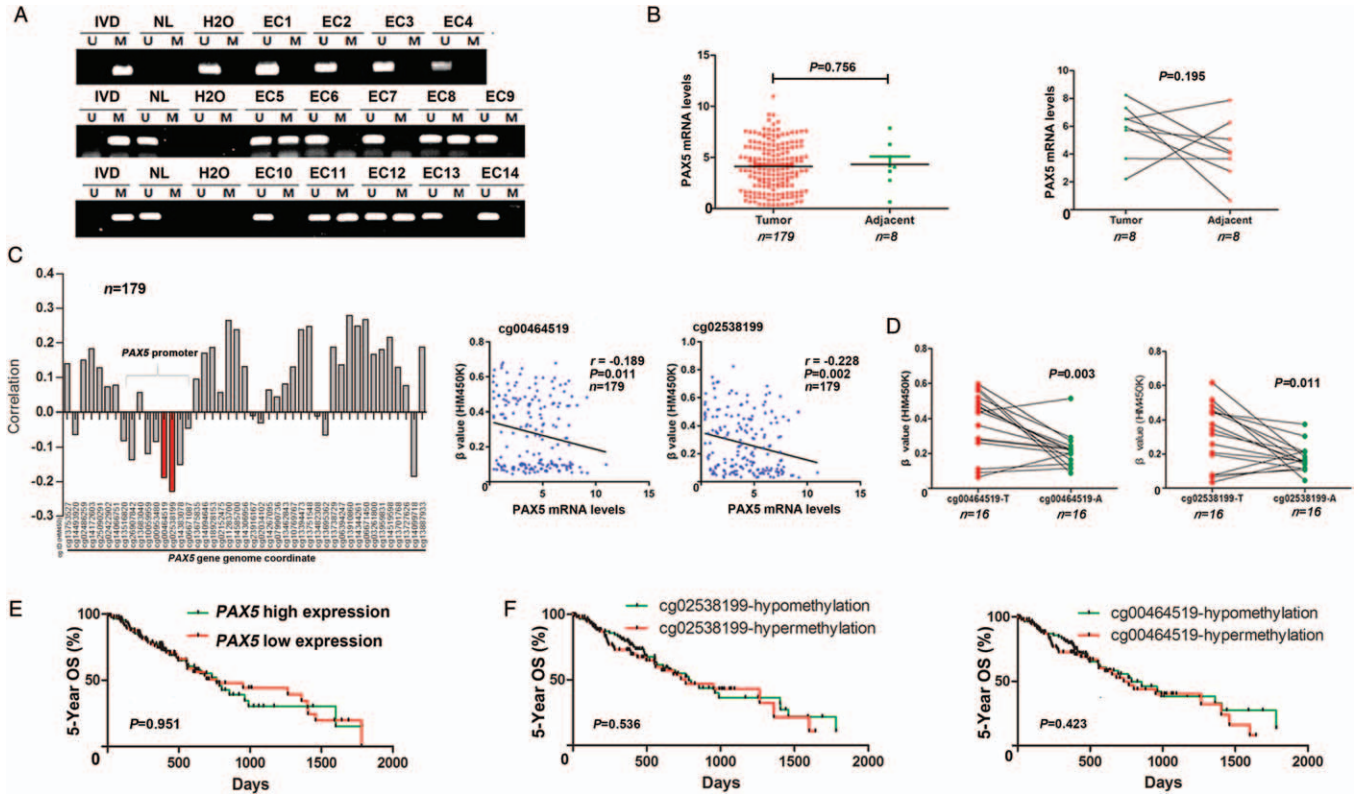

Figure 2: Expression and methylation status of *PAX5* in ESCC tissues. (A) Representative MSP results of the *PAX5* promoter region methylation status in NE mucosa and ESCC tissues. Primer efficiency was confirmed using IVD as a positive control and NL DNA as a negative control. (B) Left: Univariable scatter plots of *PAX5* mRNA expression levels in ESCC tissues ($n = 179$) *vs.* adjacent tissue samples ($n = 8$) using RNA-Seq data from TCGA and GTEx databases. *PAX5* mRNA expression (vertical axis) is expressed as log 2 (TPM + 1), where TPM is the value of transcripts per million (reads). Right: Expression of *PAX5* in eight cases of ESCC cancer tissues compared with paired adjacent tissue samples. $P > 0.05$ for both unpaired and paired samples. (C) The methylation status of the top two CpG sites (cg00464519 and cg02538199, respectively) was negatively correlated with the loss or reduction of *PAX5* expression in 179 cases of ESCC (all $P < 0.05$). (D) Methylation levels of cg00464519 and cg02538199 in the *PAX5* promoter were significantly different between ESCC tissues (T) and adjacent tissue samples (A) ($P < 0.05$). (E) Kaplan–Meier curves showed the association of the 5-year OS of ESCC patients with *PAX5* mRNA expression ($P > 0.05$). (F) Kaplan-Meier curves showed the association of 5-year OS ($n = 181$) in ESCC patients with the methylation status of *PAX5* promoter in the two CpG sites, cg02538199 and cg00464519. CpG: Cytosine guanine dinucleotide; ESCC: Esophageal squamous cell cancer; GTEx: Genotype-Tissue Expression; IVD: *In vitro*-methylated DNA; M: Methylated band; mRNA: Messenger RNA; MSP: Methylation-specific polymerase chain reaction; NE: Normal esophageal; NL: Normal lymphocyte; OS: Overall survival; *PAX5*: Paired box 5; U: Unmethylated band.

Table 1: Clinicopathological features and methylation status of the *PAX5* gene promoter region of EC patients ($n = 51$).

Clinical parameters	N	*PAX5* promoter region methylation status		χ^2	*P* values
		Methylated ($n = 19$)	Unmethylated ($n = 32$)		
Age (years)					
≤60	20	12	8	7.282	0.007
>60	31	7	24		
Sex					
Male	36	14	22	0.140	0.709
Female	15	5	10		
Tumor location					
Upper	9	3	6	0.819	0.664
Middle	31	13	18		
Lower	11	3	8		
Tumor stage					
I–II	30	7	23	6.041	0.014
III	21	12	9		

EC: Esophageal cancer; *PAX5*: Paired box 5.

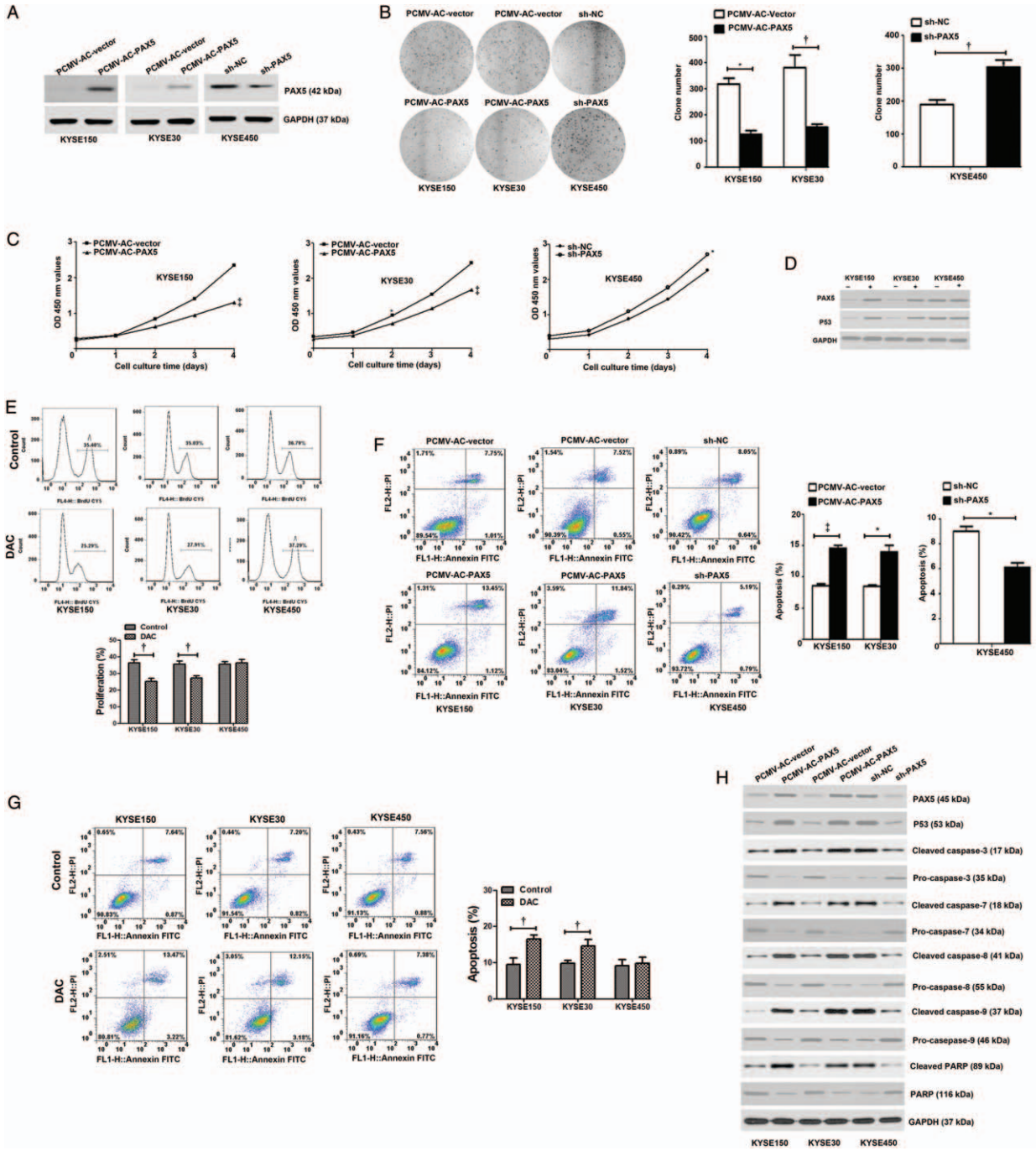

Figure 3: Effect of *PAX5* on the proliferation and apoptosis of ESCC cells. (A) Representative WBs showing the efficiency of ectopic expression of *PAX5* in KYSE150/KYSE30 cells and *PAX5* knockdown in KYSE450 cells. (B) Effects of *PAX5* on colony formation in KYSE150 and KYSE30 cell lines before and after restoration of *PAX5* expression and in KYSE450 cells with or without *PAX5* knockdown. (C) Growth curves, which were measured by MTT assays for 96 h, illustrated the effect of *PAX5* on proliferation before and after restoration of *PAX5* expression in KYSE150 and KYSE30 cells, and in KYSE450 cell lines before and after *PAX5* knockdown. (D) WBs showing the effect of DAC on expression of *PAX5* and p53 in KYSE150, KYSE30, and KYSE450 cells. (E) KYSE150, KYSE30, and KYSE450 cells were cultured for 72 h. BrdU incorporation was then evaluated using a FITC BrdU Flow Kit and analyzed by flow cytometry at 72 h after seeding. (F) Flow cytometry results of the effect of *PAX5* on apoptosis. Percentages of apoptotic cells among KYSE150 and KYSE30 cells before and after restoration of *PAX5* and in KYSE450 cells before and after *PAX5* knockdown are shown. (G) Flow cytometry results of the effect of DAC on apoptosis. Percentages of apoptotic cells among KYSE150, KYSE30, and KYSE450 cells before and after DAC treatment are shown. (H) Representative WB results of the expression levels of PAX5, p53, and apoptosis-related proteins before and after restoration of *PAX5* expression in KYSE150 and KYSE30 cell lines and before and after *PAX5* knockdown in the KYSE450 cell line. Apoptosis-related proteins include cleaved caspase-3, cleaved caspase-7, cleaved caspase-8, cleaved caspase-9, cleaved PARP, pro-caspase-3, pro-caspase-7, pro-caspase-8, pro-caspase-9, and PARP. GAPDH served as a control. $^{*}P < 0.01$, $^{\dagger}P < 0.05$, $^{\ddagger}P < 0.001$. BrdU: Bromodeoxyuridine; CY5: Sulfo-cyanine5 carboxylic acid; DAC: 5-aza-2-deoxycytidine; ESCC: Esophageal squamous cell cancer; FITC: Fluorescein isothiocyanate; FL1-H: Fluorescence 1-height; FL2-H: Fluorescence 2-height; FL4-H: Fluorescence 4-height; GAPDH: Glyceraldehyde-3-phosphate dehydrogenase; MTT: 3-(4,5-dimethyl-2-thiazolyl)-2,5-diphenyl-2-H-tetrazolium bromide; NC: Negative control; *PAX5*: Paired box 5; PARP: Poly (adenosine diphosphate-ribose) polymerase; PI: Propidium Iodide; sh: Short hairpin; WBs: Western blots.

To evaluate the effect of *PAX5* on apoptosis in ESCC cell lines, flow cytometry was used. The ratios of apoptotic cells were (14.55 ± 0.79)% *vs.* (8.54 ± 0.56)% among KYSE150 cells ($P < 0.001$) and (13.96 ± 1.84)% *vs.* (8.47 ± 0.37)% among KYSE30 cells ($P = 0.007$) with or without re-expressed *PAX5*. In KYSE450 cells that highly expressed *PAX5*, the ratio of apoptotic cells was (6.09 ± 0.64)% *vs.* (9.01 ± 0.66)% with or without knockdown of *PAX5* ($P = 0.005$) [Figure 3F]. Additionally, we found that the ratios of apoptotic cells were higher among KYSE150 and KYSE30 cells after DAC treatment compared with control groups ([16.53 ± 1.05]% *vs.* [9.47 ± 1.80]% for KYSE150, $P = 0.028$; [14.56 ± 1.77]% *vs.* [9.76 ± 0.80]% for KYSE30, $P = 0.049$), whereas no significant difference was found in KYSE450 cells with or without DAC treatment ([9.77 ± 1.69]% *vs.* [9.15 ± 1.62]%, $P = 0.804$) [Figure 3G]. Furthermore, WB was used to measure the expression levels of active and inactive forms of apoptosis-related enzymes caspase-3, caspase-7, caspase-8, caspase-9, and poly (ADP-ribose) PARP. As shown in Figure 3H, re-expression of *PAX5* in KYSE150 and KYSE30 cells increased the levels of the active forms of all five apoptosis-related enzymes. Simultaneously, the expression levels of pro-caspase-3, pro-caspase-7, pro-caspase-8, and pro-caspase-9, the inactive pro-protein forms of the apoptosis-related enzymes, and full-length PARP, were decreased significantly in *PAX5*-restored KYSE150 and KYSE30 cells. Additionally, knockdown of *PAX5* in KYSE450 cells induced significant decreases in cleaved caspase-3, cleaved caspase-7, cleaved caspase-8, cleaved caspase-9, and cleaved PARP, with increases of pro-caspase-3, pro-caspase-7, pro-caspase-8, pro-caspase-9, and full-length PARP. p53 protein was also upregulated in *PAX5*-re-expressed KYSE150 and KYSE30 cells, and down-regulated in *PAX5* knockdown KYSE450 cells [Figure 3H]. These results suggested that *PAX5* facilitated the processing of inactive caspase-3/7/8/9 (pro-caspase-3/7/8/9) into active forms (cleaved caspase-3/7/8/9) with the cleaved/full-length ratio of PARP increasing significantly, which promoted apoptosis of the ESCC cells.

PAX5 inhibits ESCC cell xenograft growth in mice

To evaluate the *in vivo* tumor-suppressive effect of *PAX5* on ESCC, we employed an ESCC cancer cell-xenografted mouse model. KYSE150 or KYSE30 cells stably transfected with *PAX5* or the empty control viral vector were injected subcutaneously into nude mice and growth curves of the subcutaneous tumor *in vivo* were constructed. As a result, an approximately 43% reduction in the tumor volume was seen after restoration of *PAX5* expression in KYSE150 cell xenografts (429.23 ± 36.01 mm^3 *vs.* 751.20 ± 131.63 mm^3; $P = 0.015$) [Figure 4A]. Similarly, an approximately 36% reduction in tumor volume was seen in *PAX5*-transfected KYSE30 cell xenografts compared with the vector control group (374.97 ± 87.93 mm^3 *vs.* 589.87 ± 118.67 mm^3; $P = 0.027$) [Figure 4B]. Following euthanization of the mice at 36 days post-transplantation, tumors were isolated and weighed. The average tumor weight was 133.07 ± 7.35 mg *vs.* 230.78 ± 7.83 mg for *PAX5*-restored KYSE150 cell xenografts and the vector control group, respectively ($P < 0.001$) [Figure 4A]. Similarly, in KYSE30 cell xenografts with or without restored *PAX5*, the average tumor weight was 92.12 ± 10.38 mg *vs.* 185.34 ± 9.49 mg ($P < 0.001$) [Figure 4B]. Both the tumor volume and weight in mice transfected with *PAX5* were significantly decreased compared with those in control mice. Furthermore, we quantified apoptosis in the xenografted tumors by TUNEL assays. Xenografted tumors in the *PAX5* group had significantly more apoptotic cells compared with those in the control group (KYSE150: [62.92 ± 4.56]% *vs.* [26.58 ± 2.93]%, $P < 0.001$; KYSE30: [44.50 ± 5.14]% *vs.* [17.84 ± 2.98]%, $P = 0.001$) [Figure 4C]. Expression of PAX5 and p53 protein in xenografts was confirmed by IHC staining, and expression of PAX5 was positively correlated with that of p53 [Figure 4D and 4E]. Thus, *PAX5* promoted apoptosis *in vivo*. In summary, these results provide *in vivo* evidence that *PAX5* acts as a tumor-suppressor gene in ESCC.

Tumor-suppressor properties of PAX5 are mediated by the p53 signaling pathway

To evaluate the effect of *PAX5* on p53 signaling in ESCC, we used a p53 dual-luciferase reporter assay. Ectopic expression of *PAX5* increased luciferase activity of the p53 reporter in both KYSE150 and KYSE30 cells (5.11 ± 0.19 *vs.* 1.00 ± 0.12, $P < 0.001$ for KYSE150 and 3.19 ± 0.48 *vs.* 1.00 ± 0.11, $P = 0.002$ for KYSE30) [Figure 5A], and, as expected, this was associated with increased p53 protein expression [Figure 5B].

To further investigate the underlying mechanism of the observed *PAX5*-mediated p53 activation, a ChIP assay using a specific anti-PAX5 antibody was employed to clarify whether *PAX5* increased p53 expression by transcriptional regulation through direct binding to the promoter region. As a result, the ChIP-qPCR assay indicated that PAX5 was bound to the p53 gene promoter [Figure 5C]. Enhanced expression of p53 at the mRNA level was confirmed by quantitative RT-PCR with more than five-fold higher expression in *PAX5*-transfected KYSE150 cells than in the vector control group (6.38 ± 0.33 *vs.* 0.98 ± 0.18, $P < 0.001$). Similar results were obtained in KYSE30 cells with approximately four-fold higher expression in *PAX5*-transfected cells *vs.* the vector control group (5.14 ± 0.47 *vs.* 1.05 ± 0.15, $P < 0.001$). Consistent with these results, knockdown of *PAX5* in KYSE450 cells led to a more than 80% reduction in p53 mRNA expression (1.01 ± 0.14 *vs.* 8.25 ± 0.86, $P < 0.001$) [Figure 5D]. These results indicated that *PAX5* regulated p53 signaling in ESCC cells at the transcriptional level. Taken together with the other findings, *PAX5* may suppress carcinogenesis of ESCC by promoting the p53 signaling pathway.

PAX5 increases the chemosensitivity of ESCC cells

To clarify whether *PAX5*-promoted apoptosis of ESCC cells enhanced the therapeutic effect of anti-cancer drugs, cell viability was assessed by MTT assays of ESCC cells with or without restored *PAX5* under treatment with docetaxel/fluorouracil (5-FU).

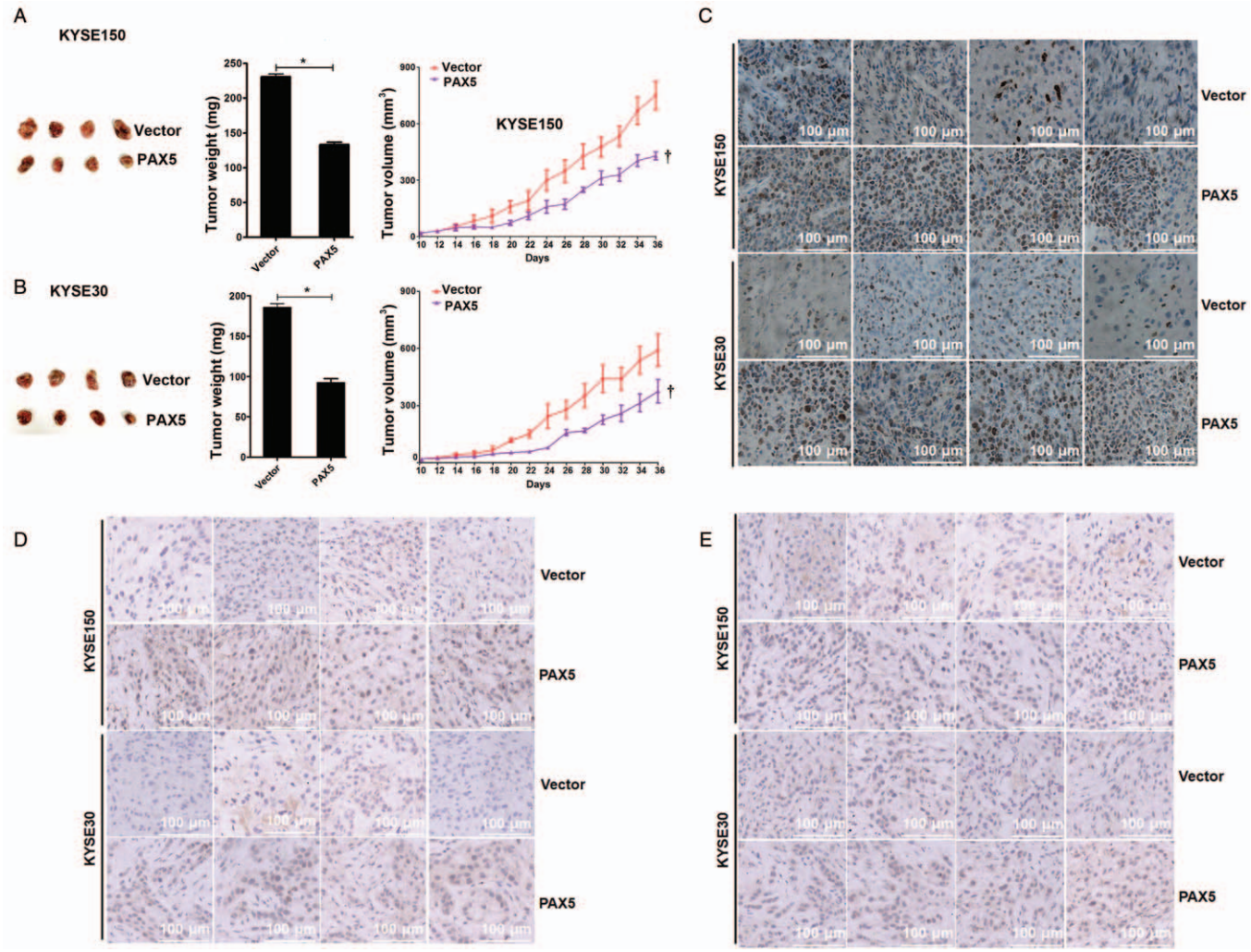

Figure 4: Effect of *PAX5* on ESCC cell xenografts. (A) Effect of *PAX5* on the growth of KYSE150 cell-xenografted tumors. Left: Representative xenografted tumors of KYSE150 cells with *PAX5* restored by a lentiviral vector *vs.* empty vector controls. Middle: Histogram of the xenograft weight in the *PAX5*-expressing group *vs.* the vector control group. Right: Growth curves of subcutaneous KYSE150 xenografted tumors from day 10 to 36. (B) Effect of *PAX5* on the growth of KYSE30 cell-xenografted tumors. (C) Representative TUNEL staining of xenografted tumors derived from KYSE150 and KYSE30 cells before and after *PAX5* transfection. The number of TUNEL-positive cells (brown-stained nuclei) was increased significantly in *PAX5*-transfected tumors (original magnification ×200). (D) Immunohistochemical staining of *PAX5* under the same conditions described in C. (E) Immunohistochemical staining of p53 under the same conditions described in C. $^{*}P < 0.001$, $^{\dagger}P < 0.05$. ESCC: Esophageal squamous cell cancer; *PAX5*: Paired box 5; TUNEL: Transferase-mediated deoxyuridinetriphate (dUTP)-digoxigenin nick end labeling.

As shown in Figure 6A, the IC_{50} of 5-FU in KYSE150 cells with restored *PAX5* and vector control cells was 15.31 ± 1.50 μmol/L *vs.* 40.83 ± 2.55 μmol/L ($P < 0.001$). Additionally, the IC_{50} in KYSE30 cells with restored *PAX5* and vector control cells was 20.26 ± 0.39 μmol/L *vs.* 38.50 ± 1.74 μmol/L ($P < 0.001$) [Figure 6A]. These results suggested that restored expression of *PAX5* sensitized ESCC cells to 5-FU. Similarly, the IC_{50} of docetaxel was approximately half with restoration of *PAX5* expression in KYSE150 and KYSE30 cells (6.48 ± 0.70 μmol/L *vs.* 10.45 ± 0.75 μmol/L in KYSE150, $P = 0.003$; 6.41 ± 0.22 μmol/L *vs.* 10.46 ± 0.84 μmol/L in KYSE30 cells, $P = 0.001$) [Figure 6B]. Consistent with these results, knockdown of *PAX5* in KYSE450 cells increased the IC_{50} values of 5-FU and docetaxel significantly (5-FU: 54.53 ± 3.14 μmol/L *vs.* 33.49 ± 1.37 μmol/L, $P = 0.004$; docetaxel: 11.84 ± 0.63 μmol/L *vs.* 6.75 ± 0.34 μmol/L, $P = 0.002$) [Figure 6C]. Furthermore, to confirm the involvement of the p53 signaling pathway in *PAX5*-induced chemosensitivity in ESCC cells, we employed pifithrin-μ, an inhibitor of p53 signaling. In *PAX5*-transfected KYSE150 cells, the IC_{50} of 5-FU in cells treated with pifithrin-μ was higher than that without pifithrin-μ treatment (39.34 ± 8.03 μmol/L *vs.* 25.56 ± 4.47 μmol/L, $P < 0.001$), although still lower than in vector control cells (39.34 ± 8.03 μmol/L *vs.* 53.07 ± 11.94 μmol/L, $P < 0.001$). A similar result was seen in KYSE30 cells. In *PAX5*-transfected KYSE30 cells, the IC_{50} of 5-FU in cells treated with or without pifithrin-μ was 36.59 ± 9.09 μmol/L *vs.* 25.43 ± 2.88 μmol/L ($P < 0.001$), and in vector control cells, the IC_{50} of 5-FU was 48.51 ± 9.61 μmol/L, which was higher than both of the above two groups ($P < 0.001$) [Figure 6D]. Similarly, the IC_{50} of docetaxel was higher in *PAX5*-transfected ESCC cells treated with pifithrin-μ than in those without pifithrin-μ treatment (8.77 ± 1.30 μmol/L *vs.* 4.57 ± 0.65

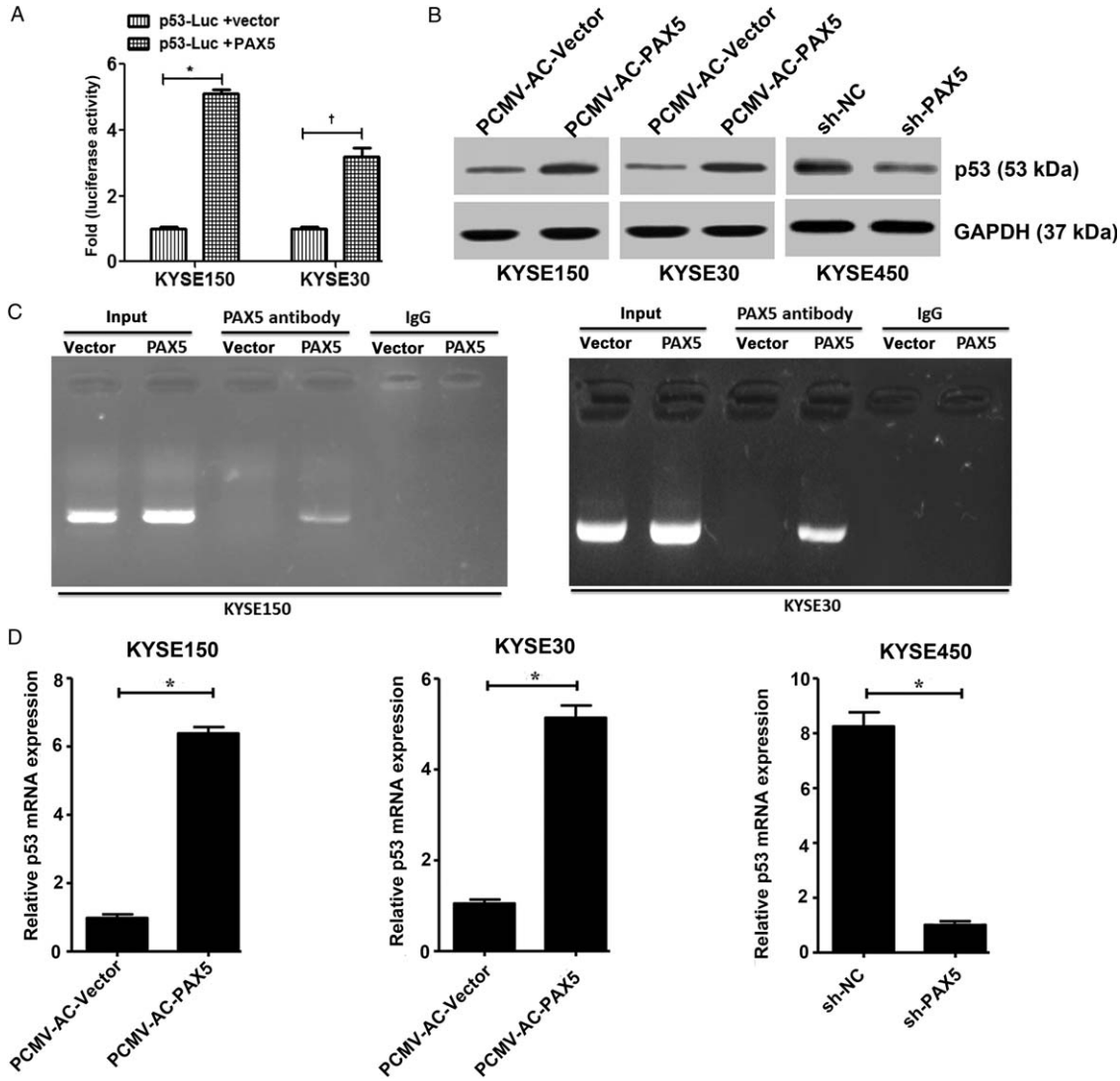

Figure 5: *PAX5* promotes p53 signaling activity in ESCC cells. (A) Results of the promoter-luciferase assay (p53-luc) in *PAX5*-stably-transfected KYSE150 and KYSE30 cells and in vector control cells. Luciferase activity was determined by the dual luciferase assay system at 48 h post-transfection. (B) Representative WBs showing the levels of p53 protein before and after *PAX5* transfection in KYSE150 and KYSE30 cell lines and in KYSE450 cells with or without *PAX5* knockdown. (C) Results of ChIP assays to investigate whether PAX5 protein bound to the promoter region of the p53 gene. Before and after *PAX5* transfection in KYSE150 and KYSE30 cell lines, soluble chromatin was immunoprecipitated with an anti-PAX5 antibody. (D) Quantitative RT-PCR showing p53 mRNA levels in KYSE150 and KYSE30 before and after *PAX5* transfection and in KYSE450 cells with or without *PAX5* knockdown. $^{*}P < 0.001$, $^{\dagger}P < 0.05$. ChIP: Chromatin immunoprecipitation; ESCC: Esophageal squamous cell cancer; GAPDH: Glyceraldehyde-3-phosphate dehydrogenase; IgG: Immunoglobin G; NC: Negative control; PAX5: Paired box 5; Sh: Short hairpin; WBs: Western blot.

μmol/L in KYSE150, $P < 0.001$; 7.83 ± 0.83 μmol/L *vs.* 4.76 ± 0.42 μmol/L in KYSE30, $P < 0.001$), although this was still lower than in the control vector group (8.77 ± 1.30 μmol/L *vs.* 12.33 ± 2.16 μmol/L, $P < 0.001$ in KYSE150 and 7.83 ± 0.83 μmol/L *vs.* 10.13 ± 1.64 μmol/L, $P < 0.001$ in KYSE30) [Figure 6E]. The results showed that pifithrin-μ as an inhibitor of p53 signaling impaired the effect of *PAX5* on chemosensitization. This suggested that *PAX5*-induced activation of p53 signaling and consequent apoptosis may increase chemosensitivity of ESCC cells.

Discussion

The *PAX5* gene is a member of a family of nuclear transcription factors named paired box genes and is located on chromosome 9p13.[36] As an activator, *PAX5* plays an important role in the development of B lymphoid cells. In B-cell precursor acute lymphoblastic leukemia, *PAX5* is a commonly altered gene and a site of genetic lesions.[37] The silencing of *PAX5* induced by promoter hypermethylation is found in several kinds of cancers including hepatocellular carcinoma,[24] gastric carcinoma,[21,22] lung cancer,[27-30] and breast cancer.[25,26] In breast cancer, *PAX5* inhibits epithelial-to-mesenchymal transition.[25,26] Hypermethylation of *PAX5* has also been reported in EC, which is associated with poor clinical outcomes and cisplatin resistance.[31] Nevertheless, its exact role and involvement in ESCC remain poorly understood.

In liver cancer, cell growth is impeded by *PAX5* via activation of the p53 signaling pathway.[24,32] In this

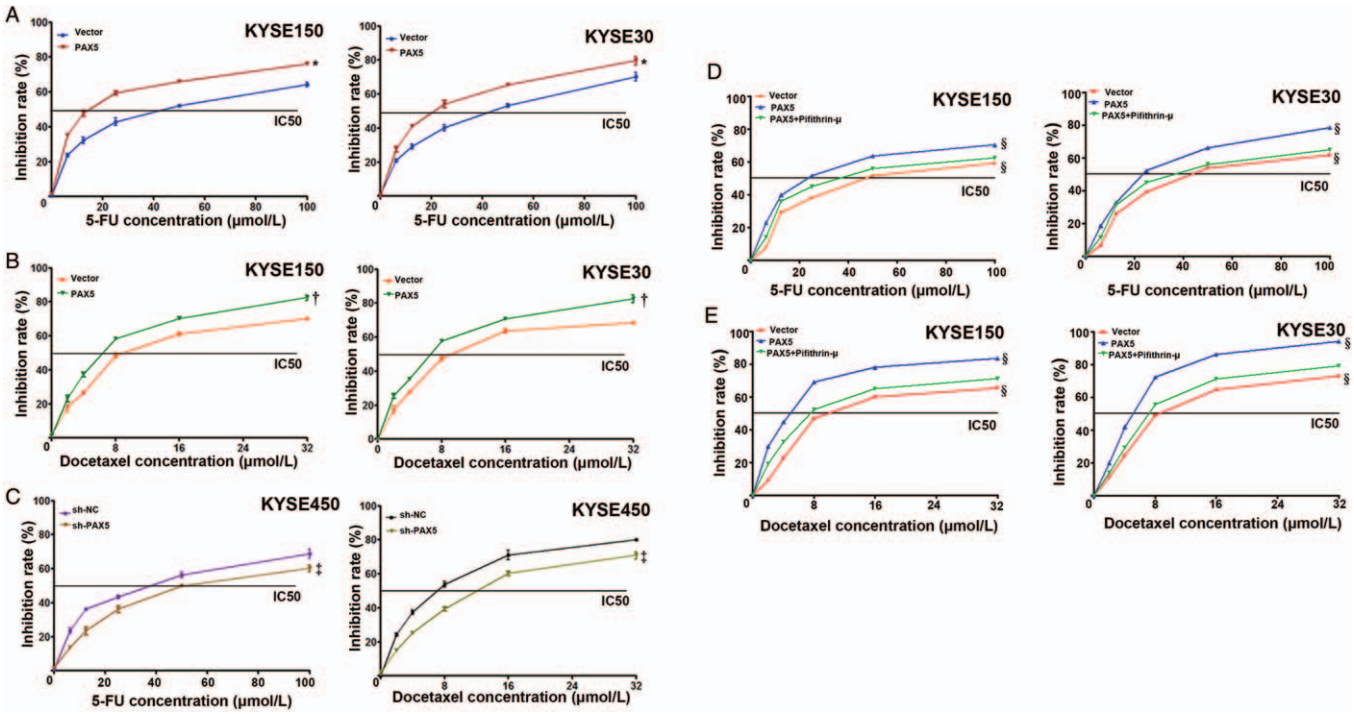

Figure 6: Effect of *PAX5* on chemosensitivity of ESCC cells to 5-FU and docetaxel. (A) Representative curves of the growth inhibition effects of 5-FU at various concentrations (0, 6.25, 12.50, 25, 50, and 100 μmol/L) in KYSE150 and KYSE30 cells with or without restoration of *PAX5* expression. (B) Representative curves of the growth inhibition effects of docetaxel at various concentrations (0, 2, 4, 8, 16, and 32 μmol/L). (C) Growth inhibition curves for 5-FU (left) and docetaxel (right) in KYSE450 cell, with or without *PAX5* gene knockdown. Concentration ranges are described above. Cell viability was measured by MTT assays after 5-FU/docetaxel treatment for 48 h. (D) Representative curves of the growth inhibition effects of 5-FU at various concentrations (0, 6.25, 12.50, 25, 50, and 100 μmol/L) in KYSE150 and KYSE30 cells before and after restoration of *PAX5* expression with or without p53 inhibitor pifithrin-μ. (E) Representative curves of the growth inhibition effects of docetaxel at various concentrations (0, 2, 4, 8, 16, and 32 μmol/L). Cell viability was measured by MTT assays after 5-FU/docetaxel treatment for 48 h. $^{*}P < 0.001$ *vs.* vector, $^{\dagger}P < 0.01$ *vs.* vector, $^{\ddagger}P < 0.001$ *vs.* sh-NC, $^{\S}P < 0.001$ *vs.* PAX5 + Pifithrin-μ. 5-FU: fluorouracil; ESCC: Esophageal squamous cell cancer; IC_{50}: Half maximal inhibitory concentration; MTT: 3-(4,5-dimethylthiazol-2-yl)-2,5-diphenyltetrazolium bromide; *PAX5*: Paired box 5.

study, we found that methylation of *PAX5* promoter region in 7/8 of ESCC cell lines was correlated with loss or reduction of *PAX5* expression, which was restored by demethylation agent DAC. Kurimoto *et al*[31] showed that ESCC patients with a high quantitative methylation-specific PCR value of *PAX5* promoter region have significantly lower rates of RFS and OS. Consistently, in our study, *PAX5* methylation was seen in 37.3% (19/51) of primary ESCC specimens by MSP detection, and the methylation was significantly associated with age ($P < 0.01$) and TNM stage ($P < 0.05$). Furthermore, by searching TCGA data, we found that *PAX5* expression was negatively correlated with promoter methylation. Nevertheless, perhaps because of the limitation in the sample size of adjacent tumor tissues as well as the cutoff value, no association was found between low expression of *PAX5* and poor 5-year OS.

Apoptosis is an important phenomenon in cytotoxicity induced by anti-cancer drugs.[38] In this study, ectopic expression of *PAX5* via lentiviral infection suppressed the growth of ESCC both *in vitro* and *in vivo*. Additionally, *PAX5* activated the p53 signaling pathway by transcriptional upregulation of p53 expression, which contributed to inhibition of ESCC cell proliferation and promotion of apoptosis. The *TP53* gene, which encodes the p53 protein, is a tumor suppressor that is mutated in numerous malignancies that include ESCC.[39,40] Increased p53 expression increases chemosensitivity,[41,42] which is a potential therapeutic target for human cancer.[43] We further explored the effect of *PAX5* on chemosensitivity and found that restoration of *PAX5* expression in ESCC cell lines increased the chemosensitivity of ESCC cells to 5-FU and docetaxel, the two main chemotherapeutic drugs used for ESCC treatment.[44]

Our results revealed that *PAX5* is a tumor suppressor in ESCC, which inhibits tumor growth by promoting the p53 signaling pathway through transcriptional upregulation of P53 protein, resulting in enhanced chemosensitivity of ESCC cells to anti-cancer drugs.

To summarize, *PAX5* is a tumor suppressor that inhibits ESCC cell proliferation, promotes apoptosis, suppresses ESCC cell xenograft growth, and increases the sensitivity of ESCC cells to chemotherapeutic agents by activating the p53 signaling pathway. Epigenetic silencing of *PAX5* contributes to progression of ESCC. *PAX5* is a novel therapeutic target and chemosensitivity biomarker for ESCC treatment.

Acknowledgements

The authors thank Mitchell Arico from Liwen Bianji (Edanz) (https://www.liwenbianji.cn) for editing the language of a draft of this manuscript.

Funding

This work was supported by grants from the National Science Foundation of China (NSFC Nos. 31671298, 81802390, and 81672462), the Natural Science Foundation of Beijing (No. 7202187), the National Key Research and Development Program of China (Nos. 2016YFC0905200, 2016YFC0905302, and 2017YFC 1308900), the National Geriatrics Center Funding (No. NCRCG-PLAGH-2018002), and the Key Projects of Clinical Application and Promotion with Capital Characteristics (No. Z161100000516003) and Military Medical Special Program for Youth of Chinese People's Liberation Army General Hospital (No. QNF19037).

Conflicts of interest

None.

References

1. Siegel RL, Miller KD, Jemal A. Cancer statistics, 2018. CA Cancer J Clin 2018;68:7–30. doi: 10.3322/caac.21442.
2. Bray F, Ferlay J, Soerjomataram I, Siegel RL, Torre LA, Jemal A. Global cancer statistics 2018: GLOBOCAN estimates of incidence and mortality worldwide for 36 cancers in 185 countries. CA Cancer J Clin 2018;68:394–424. doi: 10.3322/caac.21492.
3. Global Burden of Disease Cancer Collaboration; Fitzmaurice C, Allen C, Barber RM, Barregard L, Bhutta ZA, *et al*. Global, regional, and national cancer incidence, mortality, years of life lost, years lived with disability, and disability-adjusted life-years for 32 cancer groups, 1990 to 2015: a systematic analysis for the global burden of disease study. JAMA Oncol 2017;3:524–548. doi: 10.1001/jamaoncol.2016.5688.
4. Chen W, Zheng R, Baade PD, Zhang S, Zeng H, Bray F, *et al*. Cancer statistics in China, 2015. CA Cancer J Clin 2016;66:115–132. doi: 10.3322/caac.21338.
5. Berger SL, Kouzarides T, Shiekhattar R, Shilatifard A. An operational definition of epigenetics. Genes Dev 2009;23:781–783. doi: 10.1101/gad.1787609.
6. Hasina R, Surati M, Kawada I, Arif Q, Carey GB, Kanteti R, *et al*. O-6-methylguanine-deoxyribonucleic acid methyltransferase methylation enhances response to temozolomide treatment in esophageal cancer. J Carcinog 2013;12:20. doi: 10.4103/1477-3163.120632.
7. Yun T, Liu Y, Gao D, Linghu E, Brock MV, Yin D, *et al*. Methylation of CHFR sensitizes esophageal squamous cell cancer to docetaxel and paclitaxel. Genes Cancer 2015;6:38–48. doi: 10.18632/genesandcancer.46.
8. Chang WL, Lai WW, Kuo IY, Lin CY, Lu PJ, Sheu BS, *et al*. A six-CpG panel with DNA methylation biomarkers predicting treatment response of chemoradiation in esophageal squamous cell carcinoma. J Gastroenterol 2017;52:705–714. doi: 10.1007/s00535-016-1265-2.
9. Greenberg MVC, Bourc'his D. The diverse roles of DNA methylation in mammalian development and disease. Nat Rev Mol Cell Biol 2019;20:590–607. doi: 10.1038/s41580-019-0159-6.
10. Ahrens TD, Werner M, Lassmann S. Epigenetics in esophageal cancers. Cell Tissue Res 2014;356:643–655. doi: 10.1007/s00441-014-1876-y.
11. Baba Y, Watanabe M, Baba H. Review of the alterations in DNA methylation in esophageal squamous cell carcinoma. Surg Today 2013;43:1355–1364. doi: 10.1007/s00595-012-0451-y.
12. Li JS, Ying JM, Wang XW, Wang ZH, Tao Q, Li LL. Promoter methylation of tumor suppressor genes in esophageal squamous cell carcinoma. Chin J Cancer 2013;32:3–11. doi: 10.5732/cjc.011.10381.
13. Jia Y, Yang Y, Brock MV, Cao B, Zhan Q, Li Y, *et al*. Methylation of TFPI-2 is an early event of esophageal carcinogenesis. Epigenomics 2012;4:135–146. doi: 10.2217/epi.12.11.
14. Hoshimoto S, Takeuchi H, Ono S, Sim MS, Huynh JL, Huang SK, *et al*. Genome-wide hypomethylation and specific tumor-related gene hypermethylation are associated with esophageal squamous cell carcinoma outcome. J Thorac Oncol 2015;10:509–517. doi: 10.1097/JTO.0000000000000441.
15. Bao Y, Wang Q, Guo Y, Chen Z, Li K, Yang Y, *et al*. PRSS8 methylation and its significance in esophageal squamous cell carcinoma. Oncotarget 2016;7:28540–28555. doi: 10.18632/oncotarget.8677.
16. Issa JPJ. DNA methylation as a therapeutic target in cancer. Clin Cancer Res 2007;13:1634–1637. doi: 10.1158/1078-0432.CCR-06-2076.
17. Takeshima H, Yamada H, Ushijima T. Dammacco F, Silvestris F. Cancer epigenetics: aberrant DNA methylation in cancer diagnosis and treatment. Oncogenomics from Basic Research to Precision Medicine Salt Lake City: Academic Press; 2019;65–76.
18. Gonzalez-Fierro A, Duenas-Gonzalez A. Emerging DNA methylation inhibitors for cancer therapy: challenges and prospects. Exp Rev Precision Med Drug Dev 2019;4:27–35. doi: 10.1080/23808993.2019.1571906.
19. Cobaleda C, Schebesta A, Delogu A, Busslinger M. Pax5: the guardian of B cell identity and function. Nat Immunol 2007;8:463–470. doi: 10.1038/ni1454.
20. Dang J, Wei L, de Ridder J, Su X, Rust AG, Roberts KG, *et al*. PAX5 is a tumor suppressor in mouse mutagenesis models of acute lymphoblastic leukemia. Blood 2015;125:3609–3617. doi: 10.1182/blood-2015-02-626127.
21. Li X, Cheung KF, Ma X, Tian L, Zhao J, Go MYY, *et al*. Epigenetic inactivation of paired box gene 5, a novel tumor suppressor gene, through direct upregulation of p53 is associated with prognosis in gastric cancer patients. Oncogene 2012;31:3419–3430. doi: 10.1038/onc.2011.511.
22. Deng J, Liang H, Zhang R, Dong Q, Hou Y, Yu J, *et al*. Applicability of the methylated CpG sites of paired box 5 (PAX5) promoter for prediction the prognosis of gastric cancer. Oncotarget 2014;5:7420–7430. doi: 10.18632/oncotarget.1973.
23. Hayashi M, Guerrero-Preston R, Sidransky D, Koch WM. Paired box 5 methylation detection by droplet digital PCR for ultra-sensitive deep surgical margins analysis of head and neck squamous cell carcinoma. Cancer Prev Res (Phila) 2015;8:1017–1026. doi: 10.1158/1940-6207.Capr-15-0180.
24. Liu W, Li X, Chu ESH, Go MYY, Xu L, Zhao G, *et al*. Paired box gene 5 is a novel tumor suppressor in hepatocellular carcinoma through interaction with p53 signaling pathway. Hepatology 2011;53:843–853. doi: 10.1002/hep.24124.
25. Moelans CB, Verschuur-Maes AHJ, van Diest PJ. Frequent promoter hypermethylation of BRCA2, CDH13, MSH6, PAX5, PAX6 and WT1 in ductal carcinoma in situ and invasive breast cancer. J Pathol 2011;225:222–231. doi: 10.1002/path.2930.
26. Ahmed MB, Nabih ES, Al-Sheeha M. PAX5α and PAX5β mRNA expression in breast Cancer: relation to serum P53 and MMP2. Egypt J Med Hum Genet 2017;18:289–294. doi: 10.1016/j.ejmhg.2017.01.001.
27. Kanteti R, Nallasura V, Loganathan S, Tretiakova M, Kroll T, Krishnaswamy S, *et al*. PAX5 is expressed in small-cell lung cancer and positively regulates c-Met transcription. Lab Invest 2009;89:301–314. doi: 10.1038/labinvest.2008.168.
28. Kolhe R, Reid MD, Lee JR, Cohen C, Ramalingam P. Immunohistochemical expression of PAX5 and TdT by Merkel cell carcinoma and pulmonary small cell carcinoma: a potential diagnostic pitfall but useful discriminatory marker. Int J Clin Exp Pathol 2013;6:142–147. doi: 10.2147/OTT.S28155.
29. Zhao L, Li S, Gan L, Li C, Qiu Z, Feng Y, *et al*. Paired box 5 is a frequently methylated lung cancer tumour suppressor gene interfering beta-catenin signalling and GADD45G expression. J Cell Mol Med 2016;20:842–854. doi: 10.1111/jcmm.12768.
30. Ren Y, Hou J, Xu A, Pan Y. Diagnostic utility of PAX2 and PAX5 in distinguishing non-small cell lung cancer from small cell lung cancer. Int J Clin Exp Pathol 2015;8:14709–14716.
31. Kurimoto K, Hayashi M, Guerrero-Preston R, Koike M, Kanda M, Hirabayashi S, *et al*. PAX5 gene as a novel methylation marker that predicts both clinical outcome and cisplatin sensitivity in esophageal squamous cell carcinoma. Epigenetics 2017;12:865–874. doi: 10.1080/15592294.2017.1365207.
32. Herman JG, Graff JR, Myohanen S, Nelkin BD, Baylin SB. Methylation-specific PCR: A novel PCR assay for methylation status of CpG islands. Proc Natl Acad Sci U S A 1996;93:9821–9826. doi: 10.1073/pnas.93.18.9821.
33. Jia Y, Yang Y, Liu S, Herman JG, Lu F, Guo M. SOX17 antagonizes WNT/β-catenin signaling pathway in hepatocellular carcinoma. Epigenetics 2010;5:743–749. doi: 10.4161/epi.5.8.13104.

34. Strom E, Sathe S, Komarov PG, Chernova OB, Pavlovska I, Shyshynova I, *et al*. Small-molecule inhibitor of p53 binding to mitochondria protects mice from gamma radiation. Nat Chem Biol 2006;2:474–479. doi: 10.1038/nchembio809.
35. Yan W, Wu K, Herman JG, Brock MV, Fuks F, Yang L, *et al*. Epigenetic regulation of DACH1, a novel Wnt signaling component in colorectal cancer. Epigenetics 2013;8:1373–1383. doi: 10.4161/epi.26781.
36. Lang D, Powell SK, Plummer RS, Young KP, Ruggeri BA. PAX genes: roles in development, pathophysiology, and cancer. Biochem Pharmacol 2007;73:1–14. doi: 10.1016/j.bcp.2006.06.024.
37. Bastian L, Schroeder MP, Eckert C, Schlee C, Tanchez JO, Kampf S, *et al*. PAX5 biallelic genomic alterations define a novel subgroup of B-cell precursor acute lymphoblastic leukemia. Leukemia 2019;33:1895–1909. doi: 10.1038/s41375-019-0430-z.
38. Kim R, Tanabe K, Uchida Y, Emi M, Inoue H, Toge T. Current status of the molecular mechanisms of anticancer drug-induced apoptosis. The contribution of molecular-level analysis to cancer chemotherapy. Cancer Chemother Pharmacol 2002;50:343–352. doi: 10.1007/s00280-002-0522-7.
39. Aubrey BJ, Strasser A, Kelly GL. Tumor-suppressor functions of the TP53 pathway. Cold Spring Harb Perspect Med 2016;6:a026062. doi: 10.1101/cshperspect.a026062.
40. Bieging KT, Mello SS, Attardi LD. Unravelling mechanisms of p53-mediated tumour suppression. Nat Rev Cancer 2014;14:359–370. doi: 10.1038/nrc3711.
41. Ye S, Shen J, Choy E, Yang C, Mankin H, Hornicek F, *et al*. p53 overexpression increases chemosensitivity in multidrug-resistant osteosarcoma cell lines. Cancer Chemother Pharmacol 2016;77:349–356. doi: 10.1007/s00280-015-2944-z.
42. Lonning PE, Knappskog S. Chemosensitivity and p53; new tricks by an old dog. Breast Cancer Res 2012;14:325. doi: 10.1186/bcr3326.
43. McCubrey JA, Lertpiriyapong K, Fitzgerald TL, Martelli AM, Cocco L, Rakus D, *et al*. Roles of TP53 in determining therapeutic sensitivity, growth, cellular senescence, invasion and metastasis. Adv Biol Regul 2017;63:32–48. doi: 10.1016/j.jbior.2016.10.001.
44. NCCN Clinical Practice Guidelines in Oncology (NCCN Guidelines). Esophageal and Esophagogastric Junction Cancers. Version 3. 2020. Fort Washington: National Comprehensive Cancer Network; 2020.

How to cite this article: Zhang W, Yan W, Qian N, Han Q, Zhang W, Dai G. Paired box 5 increases the chemosensitivity of esophageal squamous cell cancer cells by promoting p53 signaling activity. Chin Med J 2022;135:606–618. doi: 10.1097/CM9.0000000000002018